

Langmuir probe diagnostics of an atmospheric pressure, vortex-stabilized nitrogen plasma jet

L. Prevosto, H. Kelly, and B. R. Mancinelli

Citation: *Journal of Applied Physics* **112**, 063302 (2012); doi: 10.1063/1.4752886

View online: <https://doi.org/10.1063/1.4752886>

View Table of Contents: <http://aip.scitation.org/toc/jap/112/6>

Published by the *American Institute of Physics*

Articles you may be interested in

[Measurement of atmospheric pressure microplasma jet with Langmuir probes](#)

Journal of Vacuum Science & Technology A: Vacuum, Surfaces, and Films **34**, 051301 (2016); 10.1116/1.4959565

[On the use of the double floating probe method to infer the difference between the electron and the heavy particles temperatures in an atmospheric pressure, vortex-stabilized nitrogen plasma jet](#)

Review of Scientific Instruments **85**, 053507 (2014); 10.1063/1.4875215

[Study of dynamical behaviour of the plasma in a dc non-transferred plasma torch using fast imaging](#)

Physics of Plasmas **24**, 033506 (2017); 10.1063/1.4977914

[Application of electrostatic Langmuir probe to atmospheric arc plasmas producing nanostructures](#)

Physics of Plasmas **18**, 073505 (2011); 10.1063/1.3614538

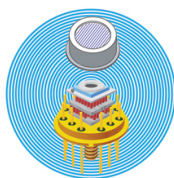
[Atmospheric pressure plasma jet in Ar and Ar/H₂O mixtures: Optical emission spectroscopy and temperature measurements](#)

Physics of Plasmas **17**, 063504 (2010); 10.1063/1.3439685

[Electric probe investigations of microwave generated, atmospheric pressure, plasma jets](#)

Journal of Applied Physics **108**, 013301 (2010); 10.1063/1.3448034

Ultra High Performance SDD Detectors



See all our XRF Solutions

Langmuir probe diagnostics of an atmospheric pressure, vortex–stabilized nitrogen plasma jet

L. Prevosto,^{1,a)} H. Kelly,^{1,2} and B. R. Mancinelli¹

¹Grupo de Descargas Eléctricas, Departamento Ingeniería Electromecánica, Facultad Regional Venado Tuerto (UTN), Laprida 651, (2600) Venado Tuerto (Santa Fe), Argentina

²Instituto de Física del Plasma (CONICET), Departamento de Física, Facultad de Ciencias Exactas y Naturales (UBA) Ciudad Universitaria Pab. I, (1428) Buenos Aires, Argentina

(Received 31 May 2012; accepted 22 August 2012; published online 19 September 2012)

Langmuir probe measurements in an atmospheric pressure direct current (dc) plasma jet are reported. Sweeping probes were used. The experiment was carried out using a dc non–transferred arc torch with a rod–type cathode and an anode of 5 mm diameter. The torch was operated at a nominal power level of 15 kW with a nitrogen flow rate of 25 NI min^{−1}. A flat ion saturation region was found in the current–voltage curve of the probe. The ion saturation current to a cylindrical probe in a high–pressure non local thermal equilibrium (LTE) plasma was modeled. Thermal effects and ionization/recombination processes inside the probe perturbed region were taken into account. Averaged radial profiles of the electron and heavy particle temperatures as well as the electron density were obtained. An electron temperature around 11 000 K, a heavy particle temperature around 9500 K and an electron density of about $4 \times 10^{22} \text{ m}^{-3}$, were found at the jet centre at 3.5 mm downstream from the torch exit. Large deviations from kinetic equilibrium were found throughout the plasma jet. The electron and heavy particle temperature profiles showed good agreement with those reported in the literature by using spectroscopic techniques. It was also found that the temperature radial profile based on LTE was very close to that of the electrons. The calculations have shown that this method is particularly useful for studying spraying–type plasma jets characterized by electron temperatures in the range 9000–14 000 K. © 2012 American Institute of Physics. [<http://dx.doi.org/10.1063/1.4752886>]

I. INTRODUCTION

Atmospheric pressure thermal plasma jets generated in direct current (dc) non–transferred arc plasma torches are used in a number of applications like plasma processing, surface modifications, spray coatings, material synthesis, and waste treatment. Standard dc non–transferred (spraying–type) plasma torches operate with a central thoriated tungsten rod–type cathode and a water–cooled annular copper anode. The plasma gas is injected into the gap between the two electrodes and serves to keep the arc root in a continuous motion over the surface of the anode. Typical torch currents are in the range of a few hundred amperes. The torch voltage depends on the nature of the plasma gas and can vary between 20 and 30 V for atomic gases up to 100 V or more when operating with molecular gases. As the gas passes around the arc through the anode–nozzle constriction, it is heated and partially ionized, emerging from the nozzle as a high–velocity plasma jet with mean temperatures of about 12 000 K and plasma velocities of a few hundred of meters per seconds.¹

Temperature measurements in non–transferred dc arc torches operated at atmospheric pressure have been obtained using both, non–invasive optical methods and enthalpy probes.^{2,3} Vardelle *et al.*,⁴ reported spectroscopic measurements using the absolute intensity method. An axial temperature of about 12 000 K was found at the nozzle exit of a

29 kW N₂/H₂ (48 NI min^{−1} 22% H₂) spraying–type torch with a 6 mm anode diameter. A similar result was reported by Scott *et al.*⁵ from the same spectroscopic technique in a 200 A Ar (30 NI min^{−1}) non–transferred dc arc torch with a 6 mm anode diameter. Joshi *et al.*,⁶ reported spectroscopic measurements using the atomic Boltzmann’s plot. The central axis value of the plasma jet temperature profile was obtained without using the Abel inversion technique.⁷ A temperature value of about 11 000 K was measured at 2 mm from the nozzle exit of a 10 kW Ar (25 NI min^{−1}) spraying–type torch with a 8 mm anode diameter. The effect of pressure on the temperature and electron density in the plasma jet of a 5 kW Ar/H₂ (15 NI min^{−1} 1% H₂) torch with a 3 mm anode diameter was experimentally investigated by Singh *et al.*⁸ using spectroscopic techniques. For a pressure of one atmosphere, an axial plasma temperature of about 11 500 K and an electron density of about $6 \times 10^{22} \text{ m}^{-3}$ were found at 4 mm downstream from the nozzle exit. Tu *et al.*,^{9,10} using a 7.3 kW Ar/N₂ (13 NI min^{−1}, 38% N₂) double–anode plasma torch, reported spectroscopic measurements of the plasma jet using the Boltzmann’s plot and the line Stark broadening. Drops in the electron temperature and electron density (from 11 300 K to 9600 K and from $6.0 \times 10^{22} \text{ m}^{-3}$ to $1.1 \times 10^{22} \text{ m}^{-3}$) were found along the torch axis at the divergent part of the first anode (5 mm diameter). Laser–scattering measurements were reported by Murphy and Kovitya¹¹ in a 200 A Ar (20 NI min^{−1}) torch with a 6 mm anode diameter. An axial temperature of about 11 000 K was found at 5 mm from the nozzle exit. All these works have assumed the

^{a)}Electronic mail: prevosto@waycom.com.ar.

validity of the local thermal equilibrium (LTE) assumption to derive the temperature from excited levels population and from the laser scattered signals (although the laser-scattering method is only slightly affected by deviations from LTE.¹¹) Besides, plasma jets are often assumed axially symmetric (regardless of the method used in the inversion process); but tomography procedures were also used. Hlína and Sonský¹² reported time-resolved tomographic measurements of temperatures in a plasma jet. They reported lack of symmetry in the cross-sectional distribution of the plasma temperature in the jet. Water cooled enthalpy probes, which considerably perturb the plasma flow (mean diameters of about 3–5 mm); were also used. Xiaozhen¹³ reported a temperature of 6600 K at 16 mm from the nozzle exit using an enthalpy probe (4.78 mm outer diameter) in a 9 kW Ar/H₂ (5% H₂) non-transferred arc plasma torch with a 5 mm anode diameter. A temperature of about 5500 K at 60 mm from the nozzle exit was reported by Kim *et al.*¹⁴ in a 120 kW Ar (200 NI min⁻¹) non-transferred arc plasma torch (well-type cathode) with 16 mm electrodes diameter.

Langmuir (electrostatic) probes are an attractive diagnostic to obtain spatially and time-resolved information on plasma parameters.^{15,16} In spite of the fact that the use of Langmuir probes was mostly restricted to low-pressure plasmas (where the collisional mean free path of charged particles is greater than the characteristic length of the probe and the perturbed region around it); they have been also employed to study high-pressure (collision-dominated) arcs.^{17–25} In particular, the ion current branch of the probe characteristic curve was frequently employed in collision-dominated arcs,^{17–22,24,25} although waveforms of the floating plasma potential signal were also analyzed.²³ However, the electrostatic probe's theory in atmospheric pressure plasmas is not well developed yet.^{15,26–29} The Langmuir probe technique in atmospheric pressure arcs was used by Gick *et al.*,¹⁷ Fanara and Richardson,¹⁸ and Fanara,^{19,20} working with tungsten inert gas (TIG) arcs; and by Prevosto *et al.*^{21–23} working with high-energy density cutting arcs. In these studies, to avoid probe damage and electron emission from the probe surface, sweeping probes have been employed. LTE was assumed in all the cases.

An experimental study of a non-transferred arc operated at atmospheric pressure using the ion branch of Langmuir probes is reported in this work. A theoretical model to explain the ion current collected by the probe through the perturbed layer surrounding the probe is also presented. This allows inferring the electron and heavy particle temperature. To our knowledge, there is no previous published works on this subject. The paper is organized as follows: the experimental set-up are described in Sec. II. The experimental results are given in Sec. III while the probe model and its results in terms of the electron and heavy particle temperature, as well as the electron density of the plasma jet are presented in Sec. IV. The conclusions are summarized in Sec. V.

II. EXPERIMENTAL SET-UP

A. Non-transferred dc arc torch

The experiment was carried out using an atmospheric pressure non-transferred dc arc torch with a water-cooled

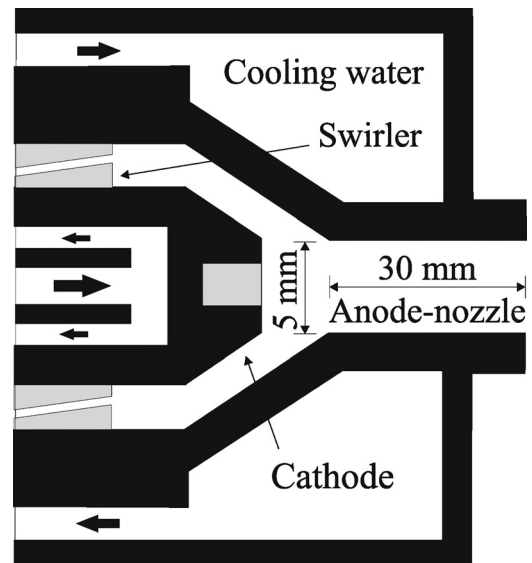


FIG. 1. Schematic of the non-transferred arc torch used in the experiment.

thoriated tungsten (2 wt. %) rod-type cathode and a water-cooled copper anode-nozzle of 5 mm internal diameter and 30 mm in length. The schematic of the torch is given in Fig. 1. The arc was vortex-stabilized and nitrogen was used as the plasma gas. The torch was operated in the so-called restrike mode^{2,3} at 15 kW (150 V, 100 A) nominal power level with a nitrogen flow rate of 25 NI min⁻¹.

B. Sweeping Langmuir probe system

The employed sweeping Langmuir probe system together with its biasing circuit is shown schematically in Fig. 2. It consisted in a rotating aluminum disk carrying one probe mounted in the radial outward direction. On one of the disc surfaces a pair of carbon brushes collected the probe current. The probes length and the disc diameter were chosen large enough in order to consider that the probe axis was approximately parallel to the line joining the jet axis to the disc center during the whole passing of the probe through the

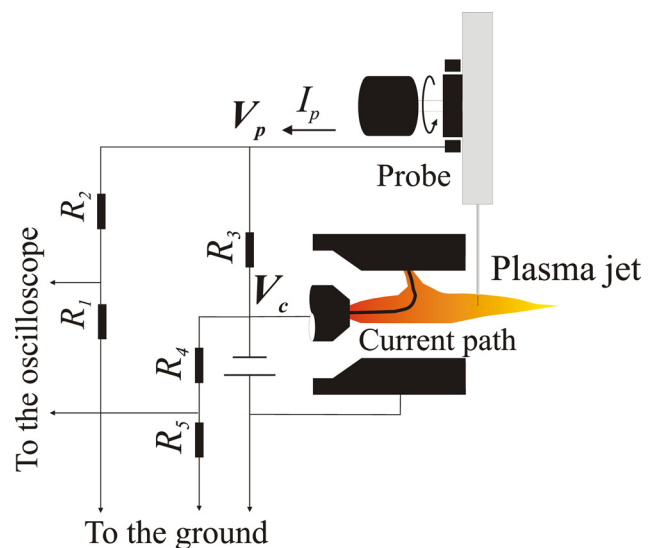


FIG. 2. Schematic of the Langmuir probe biasing circuit.

jet. The distance from the torch axis to the disc center was chosen to ensure that the probe tip swept the jet cross-section along a diameter. The measurements were obtained at 3.5 mm downstream from the torch exit. The velocity of the tip of the probes was 17 m s^{-1} . The probes were made of thin tungsten wires (radii $R_p = 100$ and $150 \mu\text{m}$) that were introduced into capillary glass tubes to insulate the metallic wires from the plasma but a certain length ($L_p = 1 \text{ mm}$) of exposed tip. The tip length was chosen large enough to reduce the edge effects, but short enough to neglect the variation of the current along the probe tip without a large error. This point will be further discussed in Sec. IV.

To obtain the ion branch of the probe characteristic curve the probes were negatively biased employing only a resistor (R_3 , see Fig. 2). In practice, R_3 was varied in the range 21–4000 Ω . For the lower R_3 values ion saturation conditions were obtained. The probe (V_p) and the arc (V_c) voltages were simultaneously measured (with respect to the grounded anode) through high-impedance voltage dividers ($R_1 = 33 \Omega$, $R_2 = 20 \text{ k}\Omega$, $R_4 = 6.7 \text{ k}\Omega$, and $R_5 = 11 \Omega$) by using a two-channel oscilloscope (Tektronix TDS 1002 B with a sampling rate of 500 MS/s and an analogical bandwidth of 60 MHz). The ion current was then obtained from

$$I_p = \left(\frac{R_1 + R_2 + R_3}{R_1 + R_2} V_p - V_c \right) \frac{1}{R_3}, \quad (1)$$

where the factor $(R_1 + R_2 + R_3)/(R_1 + R_2)$ (very close to unity for the lower values of R_3), takes into account the small current drained through the high-impedance voltage divider used to measure V_p .

The plasma fluctuations are an important characteristic of the plasma jets operated in restrike mode.^{2,3} As the probe moved relatively slowly through the jet (i.e., the probe transit time was in practice larger than the time-scale of the plasma fluctuations), the probe waveform was strongly affected by these fluctuations. Hence, the probe and arc voltage values used for the calculations were acquired using the 128 times (128 \times) average acquisition mode of the oscilloscope. Since the probe takes a time of about 5 s to traverse 128 times the arc, and this time is much larger than the typical fluctuation period (of about $70 \mu\text{s}$), this averaging mode almost quenched the arc fluctuations (mostly caused by the arc restrike). The described averaging mode is usually employed in this kind of plasma devices.²⁻⁸

More details on the employed sweeping Langmuir probe system can be found elsewhere.²¹

III. EXPERIMENTAL RESULTS

A typical (128 \times) averaged ion current waveform corresponding to a probe radius $R_p = 100 \mu\text{m}$ in ion saturation conditions ($R_3 = 21 \Omega$) is shown in Fig. 3. It can be seen that this waveform appears with a Gaussian-like shape after the quenching of the plasma fluctuation effects. Nevertheless, some fluctuation level remained present, leading to an experimental uncertainty of I_p of about 10%. No significant differences were found in the amplitude of the saturation ion current when probing the plasma jet with the larger probe.

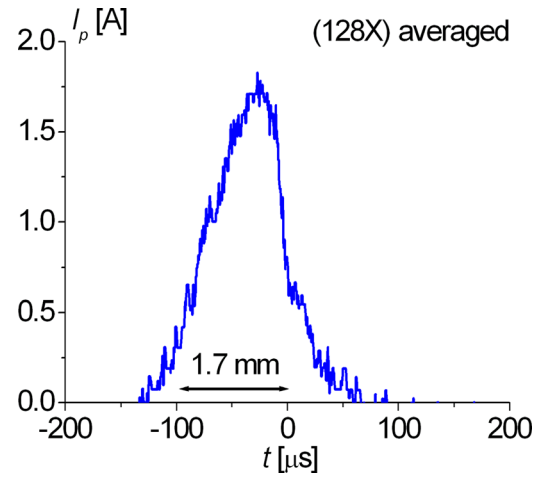


FIG. 3. Typical averaged current waveform in ion saturation conditions. $R_p = 100 \mu\text{m}$.

Using the peak values of the averaged signals, the ion branch of the current-voltage probe characteristic was built. This was done experimentally by varying the R_3 value in the probe circuit (see Fig. 2), and the obtained results are given in Fig. 4. When the probe was biased by more than -50 V (with respect to the grounded anode), a typical flat ion saturation is observed with a probe current of about 1.8 A. This feature indicates that the space-charge-layer around the probe remains thin compared to the probe radius.¹⁵

IV. INTERPRETATION OF THE RESULTS

A. The model

The ion saturation current to a non-emitting, cylindrical sweeping Langmuir probe immersed into an atmospheric pressure ambient, partially-ionized (degree of ionization of about 1%), non-equilibrium and electropositive plasma is considered. The probe is under a negative potential with respect to the undisturbed plasma (about or below the floating potential) so the electron flux is equal to or smaller than the ion flux. The model includes the following assumptions in the plasma region perturbed by the probe: (1) the ion

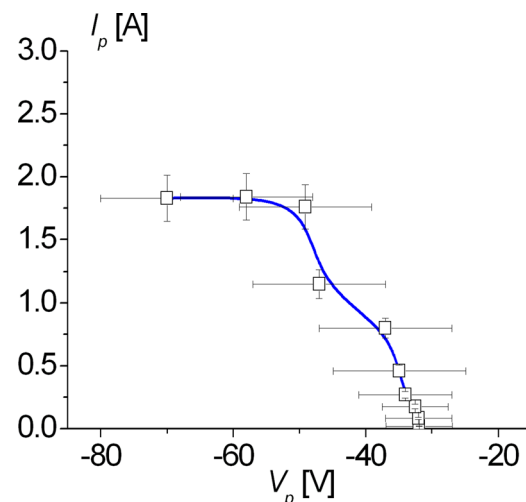


FIG. 4. Averaged probe characteristic curve. Ion branch.

current to the probe is stationary; (2) the ion convection is a minor effect relative to ion diffusion; (3) creation and removal of charged particles are minor effects relative to ion diffusion. In such a case the probe perturbed region can be divided into a collision-dominated (quasi-neutral) plasma region where strong gradients in the plasma density exists, i.e., the diffusion layer (being $\Delta \approx R_p$ its length-scale); and a thin collisionless positively charged layer located adjacent to the probe surface, the thickness of this layer (length-scale of few electron Debye radius $-\lambda_D$) being much less than the probe dimensions and the thickness of the near-probe viscous boundary layer.^{26,27,29} The structure of this the space-charge layer was not taken into account. In addition, it is considered in the quasi-neutral plasma a thermal layer (being δ its length-scale) in which the temperature of the heavy particle (T_h) is much lower than its value far away from the probe ($T_{h\infty}$).²⁸ For such layer the following assumptions are added: (4) the temperature of the heavy particle approaches linearly to the probe surface temperature (T_w); (5) the electron temperature is a constant (and equal to its value far away from the probe (T_e)). A scheme of the whole probe perturbed region is given in Fig. 5.

The assumption (1) implies in this case that the time needed for the ion flux to cover a distance Δ ($= R_p$) ($\tau_d \equiv R_p^2/D_{a\infty}$), is much smaller than the probe transit time. The assumption (2) implies that the diffusive Péclet number ($Pe \equiv v_\infty R_p/D_{a\infty}$) is smaller than unity. Δ is in this case comparable to R_p .^{26,27} The assumption (3) implies that the ionization length calculated using the equilibrium densities ($L \equiv \sqrt{D_{a\infty}/k_{rec}N^2}$) is higher than R_p .²⁶⁻²⁹ Here D_a is the ion ambipolar diffusion coefficient, v is the plasma

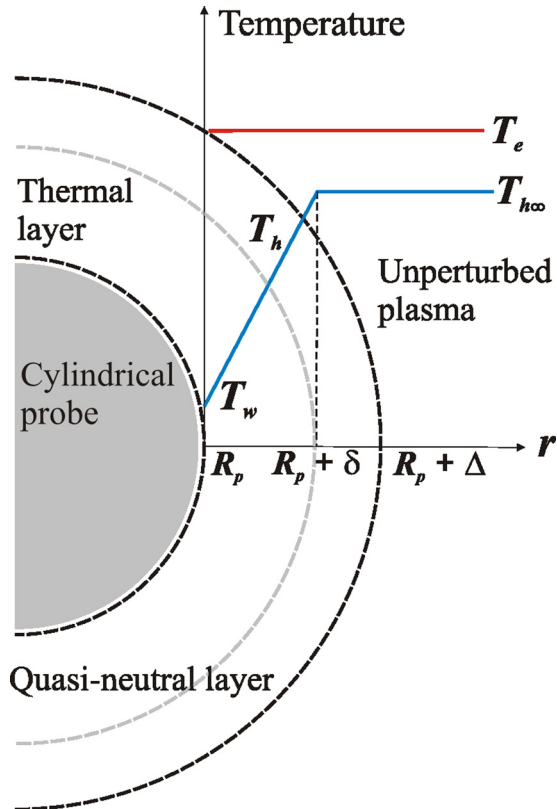


FIG. 5. Scheme of the whole probe perturbed region.

flow velocity, k_{rec} is the ion recombination coefficient, N is the electron density far away from the probe, and the subscript ∞ indicates unperturbed values. Finally, assumptions (4) and (5) take into account probe cooling effects on the adjacent plasma. In particular, the assumption (4) implies that the relaxation length of the electron energy in elastic collisions with heavy particles ($\lambda_u \equiv \lambda_{e\infty}(M/2m)^{1/2}$) is larger than δ . By equating the heat flux to the probe ($((1/r)\partial(r\kappa_h dT_h/dr)/\partial r \approx (2/3)\kappa_h(T_{h\infty} - T_w)/(R_p\delta))$) by heavy particle thermal conduction and the energy transfer to heavy particles by elastic electron-heavy particles collisions ($((3/2)k(T_e - T_w)(2m/M)Nv_{c\infty})$); the characteristic value of δ can be estimated as²⁸

$$\delta^{-1} \approx \frac{9}{4} \left(\frac{2m}{M} \right) \frac{Nv_{c\infty}kR_p}{\kappa_h} \theta, \quad (2)$$

where for simplicity T_w was neglected compared to T_e (and $T_{h\infty}$) and it was introduced the ratio $\theta \equiv T_e/T_{h\infty}$ to take into account kinetic deviations with respect to LTE. Here $\lambda_e \equiv (N_0Q^{e,0} + N_+Q^{e,+})^{-1}$ is the electron mean-free-path for elastic collisions (being, respectively, $Q^{e,0}$ and $Q^{e,+}$ the electron-neutral and electron-ion collision cross-sections, and N_+ and N_0 the ion and neutral density; respectively), m and M are the electron and heavy particle mass, respectively; r is the radial probe coordinate, κ_h is the heavy particle thermal conductivity calculated for $T_h = T_w$, k is the Boltzmann's constant and $v_c \equiv \langle v_e \rangle / \lambda_e$ is the frequency of the electron-heavy particle collisions ($\langle v_e \rangle$ is the electron thermal velocity). The validity of the above quoted assumptions will be verified later.

The value of the ion current density is determined by the ambipolar flux from the quasi-neutral region to the outer boundary of the space-charge layer²⁶⁻³⁰

$$\bar{j} = -eD_a \nabla N_+, \quad (3)$$

(e is the electron charge). Besides, for a non-LTE plasma in the presence of a collecting surface (i.e., the ions diffuse to the probe where they recombine and then diffuse as neutrals back to the plasma)²⁶⁻³⁰

$$D_a \equiv \frac{kT_h}{M'v_{+,0}} \left(1 + \frac{T_e}{T_h} \right) \lambda_+, \quad (4)$$

where $M' \approx M/2$ is the reduced mass for ion-neutral collisions, $v_{+,0} \equiv \sqrt{16kT_h/\pi M}$ is the average relative ion-neutral velocity and $\lambda_+ \equiv (Q^{+,0}(N_+ + N_0))^{-1}$ is the ion mean-free-path ($Q^{+,0}$ is the elastic ion-neutral collision cross-section).

At the outer boundary of the quasi-neutral region the ion density coincides with that of the undisturbed plasma ($N_+ \equiv N$). Since the ions leaves the quasi-neutral plasma and enter into the collisionless space-charge layer with a velocity equal to or slightly exceeding $v_B \approx (k(T_e)/M)^{1/2}$;³⁰ the ion flux at the layer entrance is given by $N_s v_B$ (being N_s the plasma density at the outer boundary of the space-charge layer). By approximating Eq. (3) as $D_{a\infty}(N - N_s)/R_p \approx N_s v_B$, N_s can be estimated as²⁸

$$N_s \approx N \frac{D_{a\infty}/R_p}{v_B + D_{a\infty}/R_p} \propto N \frac{\lambda_{+ \infty}}{R_p}. \quad (5)$$

From Eq. (5) note that N_s results rather small compared to the unperturbed plasma density N .

The formulation also includes the generalized Saha equation as derived by Van de Sanden *et al.*³¹

$$\frac{N^2}{N_0} = 2 \frac{Q_+}{Q_0} \left(\frac{2\pi m k T_e}{h^2} \right)^{3/2} \exp\left(-\frac{E_I}{k T_e}\right), \quad (6)$$

and the equation of state

$$\frac{p}{k} = (T_e + T_h)N + T_h N_0, \quad (7)$$

where Q_+ and Q_0 are the statistical weights of atomic ions and atoms, respectively; h is the Planck's constant, E_I is the first ionization energy of the atoms, and p is the pressure.

For θ close to 1 and for T_e equal or slightly above to 10 000 K the nitrogen molecules have low concentration; the main ion being the atomic.¹

Replacing Eqs. (4) and (5) into Eq. (3) and using Eq. (7) to eliminates the neutral density, and using that the ion current is constant throughout the quasi-neutral plasma region perturbed by the probe, N_+ can be integrated throughout the diffusion layer (from the outer boundary of the space-charge layer to the diffusive layer edge); to yield

$$I_p \approx 1.4 L_p e \pi^{3/2} v_B T_{h\infty}^{1/2} (T_{h\infty} + T_e) \times \sigma_{+,0}^{-1} T_e^{-3/2} \ln \left| \frac{p/k - N_s T_e}{p/k - N T_e} \right| \Lambda^{-1}, \quad (8)$$

which is the current to the probe. Λ is a dimensionless parameter given by

$$\Lambda \equiv 1.4 T_{h\infty}^{1/2} (T_{h\infty} + T_e) \int_{R_p}^{R_p + \Delta} dr / \left(r (T_e + T_h) T_h^{1/2} \right), \quad (9)$$

that takes into account the effects of the plasma cooling on the ion current, i.e., $\Lambda \equiv 1$ if the assumption of $T_h = \text{const}$ is made in the probe perturbed region. (The factor 1.4 in Eqs. (8) and (9) corresponds to an estimation of $1/\ln|1 + \Delta/R_p|$ with $\Delta/R_p \approx 1$). As N_s is rather small compared to N , I_p results almost independent of R_p in accordance with the experiment.

With all of these considerations the probe model reduces to the set of Eqs. (6)–(8), which is not closed yet, since the number of unknown plasma quantities is four (N , N_0 , T_e , and $T_{h\infty}$). To do this, it is supposed that the LTE departure can be related to the electron density N in accordance to André *et al.*^{32,33} In their papers it was assumed that

$$\theta \equiv 1 + A \ln \left| \frac{N}{N^{LTE}} \right|, \quad (10)$$

where N^{LTE} is the electron density above which LTE is assumed (i.e., $N^{LTE} \approx 10^{23} \text{ m}^{-3}$ in accordance with the Griem

criterion³⁴) and $A = -0.2$ for a dc N_2 plasma jet, in according to experimental results. Adding Eq. (10) the model is now closed with the experimental averaged data of I_p as an input. Because of the high sensitivity of the ion current to T_e in the considered range of temperatures, the uncertainty in the ion current measurement due to plasma fluctuations (mostly caused by the arc restrike) has little influence on the derived values of T_e .

To perform the inversion of Eq. (8), the probe tip length was ignored, adopting an average value of the ion current along it. The use of the Abel inversion procedure is thus avoided. Estimations based on the Eq. (8) have been shown that this approach lead to an error less than 1% at the jet axis and less than 5% at its edges for T_e .

B. Model results

Averaged radial distributions of electron and heavy particle temperatures as well as the ratio $\theta \equiv T_e/T_{h\infty}$ for the given torch operation conditions and for a distance of 3.5 mm downstream from the torch exit are shown in Fig. 6. The typical obtained uncertainties (including those due to the finite length of the probe tip) are about 6% for T_e and around 12% for $T_{h\infty}$. For comparative purposes, the temperature profile based on LTE (T) is also shown. Noticeable deviations from kinetic equilibrium in the whole radial range are observed, with a difference between the profiles of T_e and $T_{h\infty}$ reaching about 3000 K ($\theta \equiv T_e/T_{h\infty} \approx 1.4$) at the plasma edges. These electron and heavy particle temperature profiles are in good agreement with those reported by using spectroscopic methods (see for instance Fig. 11 of the review in Ref. 3) in a dc N_2 plasma jet operated at a similar power level (14 kW). It is also shown in Fig. 6 that the electron temperature remains very close to the LTE temperature, with values of around 11 000 K at the jet centre in good agreement with several reported T measurements in non-transferred arc torches.^{1–11} Since in non-LTE plasmas the atomic ionization is governed by T_e (instead of T),^{31,34} T_e results in this case almost overlapped with T .

The averaged radial distribution of the plasma density N is given in Fig. 7. In this case the typical uncertainties are

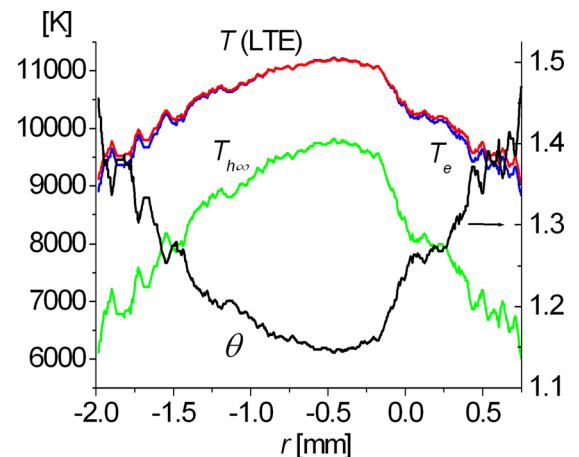


FIG. 6. Averaged radial distributions of the electron and heavy particle temperatures. The ratio θ and the LTE temperature radial profile are also shown.

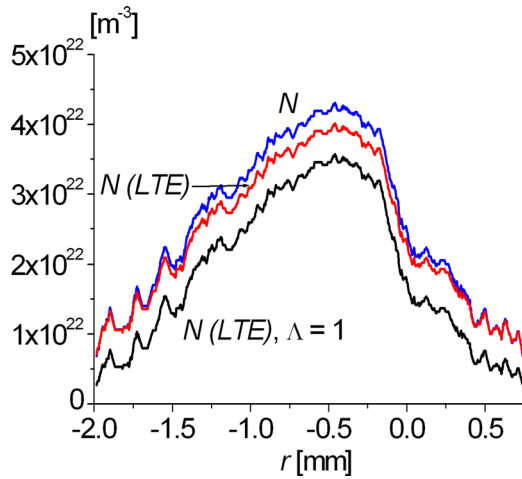


FIG. 7. Averaged radial distribution of the plasma density. For comparative purposes the corresponding LTE profiles considering the plasma cooling and for $\Lambda = 1$ (i.e., without considering plasma cooling) are also shown.

less than 30%. It can be seen that N reaches a value of around $4 \times 10^{22} \text{ m}^{-3}$ at the plasma centre; which is rather lower than the value ($\approx 10^{23} \text{ m}^{-3}$) derived from Griem's criterion for the LTE validity. For comparative purposes, the plasma density profile calculated under the LTE assumption ($N(\text{LTE})$), together with the corresponding profile but for $\Lambda = 1$ (i.e., without considering the plasma cooling by the probe) are also shown. As it can be seen, the N and $N(\text{LTE})$ profiles are close, being the largest difference (less than 10%), within the uncertainty range. On the other hand, noticeable departures from LTE (for $\Lambda = 1$) are observed in almost the whole radial range; being N higher in a factor of about 2.5 at the plasma fringes.

From the above given results, the parameter Λ (given by Eq. (9)) varies from a value close to unity (≈ 1.1 for non-LTE and ≈ 1.2 for LTE) at the jet centre (where δ is rather low compared to R_p), to a value of about 1.6 and 2, respectively, at the jet edges (where δ is comparable to R_p). In any case, due to the high sensitivity of the ion current to T_e , the error in the calculation of T_e assuming $T_h = \text{constant}$ is only of about 100 K at the jet centre and around 500 K at the periphery.

Concerning to the trend showed by the plasma density profiles in Fig. 7, the explanation is as follows. Since the electron pressure is quite small as compared to the total pressure, it results $-\ln|1 - NkT_e/p| \approx NkT_e/p$, and therefore Eq. (8) can be rewritten as $I_p \propto eL_p(D_{a\infty}/\Lambda)N$. The term $D_{a\infty}/\Lambda$ can be interpreted as the effective ion diffusion coefficient (which includes the probe cooling effects on the ion mobility). In LTE, the diffusion results higher than the corresponding value for a non-LTE plasma. This means that the reconstructed value of the plasma density results smaller if the LTE assumption is made (see the profile of $N(\text{LTE})$ for $\Lambda = 1$ in Fig. 7). However, due to the probe cooling effects, the ion temperature is depleted near the probe and the diffusion coefficient is reduced by the factor $1/\Lambda$. Since the value of $1/\Lambda$ becomes higher toward the edges under the LTE assumption, $D_{a\infty}/\Lambda$ results almost insensible to the LTE assumption; therefore, N and $N(\text{LTE})$ becomes almost overlapped.

There is an optimum electron temperature range, defined by the validity of the basic assumptions of the model, for which the present technique yields reliable results for atmospheric pressure plasma jets (as those generated by non-transferred arc torches). For low electron temperatures (slightly below 9000 K), the thermal layer thickness (estimated by Eq. (2) for $T_w \approx 1000 \text{ K}$ and $\kappa_h \approx 4 \times 10^{-2} \text{ W K}^{-1} \text{ m}^{-1}$) becomes comparable to the probe size ($R_p = 100 \mu\text{m}$ in this case) and the quasi-neutral perturbed region around it; so the necessary condition for a comprehensive use of the probe (that is: the plasma should not be perturbed sufficiently far away from the probe surface) is not accomplished in such case. Besides, as the calculation shown, below of 9000 K the ion current to the probe would be very small and strongly affected by the fluctuations. Furthermore, below of 9000 K the Péclet number (estimated for $v_\infty \approx 200 \text{ m s}^{-1}$,³⁵ and for $Q^{+,0} \approx 4 \times 10^{-19} \text{ m}^2$) results comparable to unity (due to the small value of $D_{a\infty}$); and the convective charge transport to the probe is not a minor effect compared to diffusion. On the other hand, for T_e above of 14000 K the ionization length (estimated as $L \equiv \sqrt{D_{a\infty}/k_{rec}N^2}$ for $\beta \approx 5.3 \times 10^{-23} T_e^{-9/2} \text{ m}^6 \text{ s}^{-1}$) becomes comparable to the probe size; and a ionization layer around the probe will build up in a time ($\approx (k_{rec}N^2)^{-1}$) quite high compared to the ion diffusion time ($\equiv R_p^2/D_{a\infty}$) and eventually comparable to the probe transit time. Also, above of 14000 K, the relaxation length of the electron energy (estimated as $\lambda_u \equiv \lambda_{e\infty} (M/2m)^{1/2}$ for $Q^{e,0} \approx 5 \times 10^{-20} \text{ m}^2$ and $Q^{e,+} \approx 1.9 \times 10^{-8} T_e^{-2} \text{ m}^2$) becomes comparable to the probe size, and hence the electron temperature would be depleted near the probe.

From the above estimations, a useful electron temperature range can be established. This range (9000–14 000 K for N_2) is typically found in non-transferred arc torches operated at power levels of the order of 10 kW.^{2–11}

V. CONCLUSIONS

By applying the Langmuir probe technique to an atmospheric pressure dc nitrogen plasma jet operated at a power level of 15 kW has allowed deriving the averaged radial profiles of the electron and heavy particle temperatures; as well as the electron density. Large deviations from kinetic equilibrium were found throughout the plasma jet. The electron and heavy particle temperature profiles showed good agreement with those reported in the literature by using spectroscopic techniques. It was also found that the temperature profile in the plasma jet based on LTE was very close to that of electrons. Several estimations have been shown that this method is particularly useful for studying spraying-type plasma jets characterized by electron temperatures in the range 9000–14 000 K.

ACKNOWLEDGMENTS

This work was supported by grants from the CONICET (PIP 112/20090/00219) and Universidad Tecnológica Nacional (PID-UTN 1389). H.K. and L.P. are members of the CONICET.

- ¹M. Boulos, P. Fauchais, and E. Pfender, *Thermal Plasmas, Fundamentals and Applications* (Plenum, New York, 1994), Vol. 1.
- ²P. Fauchais, *J. Phys. D: Appl. Phys.* **37**, R86 (2004).
- ³P. Fauchais and A. Vardelle, *IEEE Trans. Plasma Sci.* **25**, 1258 (1997).
- ⁴A. Vardelle, J. M. Baronnet, M. Vardelle, and P. Fauchais, *IEEE Trans. Plasma Sci.* **8**, 417 (1980).
- ⁵D. A. Scott, P. Kovitya, and G. N. Haddad, *J. Appl. Phys.* **66**, 5232 (1989).
- ⁶N. K. Joshi, S. N. Sahasrabudhe, K. P. Sreekumar, and N. Venkatramani, *Meas. Sci. Technol.* **8**, 1146 (1997).
- ⁷A. Marotta, *J. Phys. D: Appl. Phys.* **27**, 268 (1994).
- ⁸N. Singh, M. Razafinimanana, and A. Gleizes, *J. Phys. D: Appl. Phys.* **31**, 2921 (1998).
- ⁹X. Tu, B. G. Chéron, J. H. Yan, and K. F. Cen, *Plasma Source Sci. Technol.* **16**, 803 (2007).
- ¹⁰X. Tu, B. G. Chéron, J. H. Yan, L. Yu, and K. F. Cen, *Phys. Plasmas* **15**, 053504 (2008).
- ¹¹A. B. Murphy and P. Kovitya, *J. Appl. Phys.* **73**, 4759 (1993).
- ¹²H. Hlína and J. Sonský, *J. Phys. D: Appl. Phys.* **43**, 055202 (2010).
- ¹³F. Xiaozhen, *Plasma Sci. Technol.* **5**, 1909 (2003).
- ¹⁴K. S. Kim, J. M. Park, S. Choi, J. Kim, and S. H. Hong, *J. Phys. D: Appl. Phys.* **41**, 065201 (2008).
- ¹⁵Y. P. Raizer, *Gas Discharge Physics* (Springer, Berlin, Germany, 1991).
- ¹⁶N. S. J. Braithwaite and R. N. Franklin, *Plasma Sci. Technol.* **18**, 014008 (2009).
- ¹⁷A. E. F. Gick, M. B. C. Quigley, and P. H. Richards, *J. Phys. D: Appl. Phys.* **6**, 1941 (1973).
- ¹⁸C. Fanara and I. M. Richardson, *J. Phys. D: Appl. Phys.* **34**, 2715 (2001).
- ¹⁹C. Fanara, *IEEE Trans. Plasma Sci.* **33**, 1072 (2005).
- ²⁰C. Fanara, *IEEE Trans. Plasma Sci.* **33**, 1082 (2005).
- ²¹L. Prevosto, H. Kelly, and B. Mancinelli, *IEEE Trans. Plasma Sci.* **36**, 263 (2008).
- ²²L. Prevosto, H. Kelly, and F. O. Minotti, *IEEE Trans. Plasma Sci.* **36**, 271 (2008).
- ²³L. Prevosto, H. Kelly, and B. Mancinelli, *IEEE Trans. Plasma Sci.* **37**, 1092 (2009).
- ²⁴L. Prevosto, H. Kelly, and B. Mancinelli, *J. Appl. Phys.* **105**, 013309 (2009).
- ²⁵L. Prevosto, H. Kelly, and B. Mancinelli, *J. Appl. Phys.* **110**, 083302 (2011).
- ²⁶M. S. Benilov and B. V. Rogov, *J. Appl. Phys.* **70**, 6726 (1991).
- ²⁷M. S. Benilov, *J. Phys. D: Appl. Phys.* **33**, 1683 (2000).
- ²⁸V. A. Nemchinsky, *J. Phys. D: Appl. Phys.* **42**, 055205 (2009).
- ²⁹M. S. Benilov, *J. Plasma Phys.* **50**, 293 (1993).
- ³⁰M. S. Benilov and G. V. Naidis, *Phys. Rev. E* **57**, 2230 (1998).
- ³¹M. C. M. van de Sanden, P. P. J. M. Schram, A. G. Peeters, J. A. M. van der Mullen, and G. M. W. Kroesen, *Phys. Rev. A* **40**, 5273 (1989).
- ³²P. André, J. Aubreton, M. F. Elchinger, P. Fauchais, and A. Lefort, *Plasma Chem. Plasma Process.* **21**, 83 (2001).
- ³³P. André, J. Aubreton, M. F. Elchinger, P. Fauchais, and A. Lefort, *Ann. N.Y. Acad. Sci.* **891**, 81 (1999).
- ³⁴V. Rat, A. B. Murphy, J. Aubreton, M. F. Elchinger, and P. Fauchais, *J. Phys. D: Appl. Phys.* **41**, 183001 (2008).
- ³⁵J. F. Brillhac, B. Pateyron, J. F. Coudert, and P. Fauchais, in *11th (ISPC) International Symposium on Plasma Chemistry* (IUPAC, Loughborough, UK, 1993), p. 362.